JACS
JOURNAL OF THE AMERICAN CHEMICAL SOCIETY

COMMUNICATION

pubs.acs.org/JACS

Crystallographic Recognition Controls Peptide Binding for Bio-Based Nanomaterials

Ryan Coppage,[†] Joseph M. Slocik,[‡] Beverly D. Briggs,[†] Anatoly I. Frenkel,[§] Hendrik Heinz,[⊥] Rajesh R. Naik,[*,‡] and Marc R. Knecht[*,†]

[†]Department of Chemistry, University of Miami, Coral Gables, Florida 33124, United States

[‡]Nanostructured and Biological Materials Branch, Air Force Research Laboratory, Wright-Patterson Air Force Base, Ohio 45433-7702, United States

[§]Department of Physics, Yeshiva University, New York, New York 10016, United States

[⊥]Department of Polymer Engineering, University of Akron, Akron, Ohio 44325, United States

Supporting Information

ABSTRACT: The ability to control the size, shape, composition, and activity of nanomaterials presents a formidable challenge. Peptide approaches represent new avenues to achieve such control at the synthetic level; however, the critical interactions at the bio/nano interface that direct such precision remain poorly understood. Here we present evidence to suggest that materials-directing peptides bind at specific time points during Pd nanoparticle (NP) growth, dictated by material crystallinity. As such surfaces are presented, rapid peptide binding occurs, resulting in the stabilization and size control of single-crystal NPs. Such specificity suggests that peptides could be engineered to direct the structure of nanomaterials at the atomic level, thus enhancing their activity.

Nanomaterials are attractive for a variety of applications ranging from catalysis to photonics due to the enhancement of properties achieved at the nanoscale.[1] Unfortunately, few methods can accurately control particle size, structure, crystallinity, and atomic arrangement with inorganic specificity, especially at sizes <10 nm. By accessing this region, maximization of the surface-to-volume ratio can be achieved, which is important for catalytic and energy applications.[1a,d,e] To achieve this, methods must be developed that can rapidly prepare high surface area materials with precise tailoring of the ligand/inorganic interface, which is significantly involved in nanostructure functionality.[1f,2]

Bio-inspired approaches toward materials fabrication have emerged as promising methods that are energy efficient and eco-friendly.[3] We have recently shown that Pd nanoparticles (NPs) prepared using the Pd4 peptide (TSNAVHPTLRHL) are highly reactive for Stille C−C coupling,[4] where the peptide plays an intimate role in catalysis.[2a] This suggests that the peptides at the interface can be tuned to enhance activity; however, minimal experimental information is available concerning bio/inorganic nanosurface binding. Recently, facet-specific peptides have been isolated for the seed-mediated fabrication of cubic and tetrahedral Pt NPs.[5] It is likely that the peptides bind to the small seeds; however, these interactions are poorly understood where the amorphous nuclei transitions to the crystalline particle. Such sizes are attractive for applications such as catalysis to maximize the surface-to-volume ratio to efficiently display the reactive metal. Furthermore, by tuning the size of the materials, dramatic property transitions can occur; thus, it is important to understand the relationship between peptide binding/affinity and NP structure/size. Beyond the final NPs, the coordination environment before reduction may also play an important role in structure formation, which remains unexplored. Here we present evidence that indicates that the Pd4 peptide mediates the production of size-controlled, single-crystal Pd NPs, where the Pd^{2+}/peptide coordination environment plays an important role in the reduction potential of the system. The data suggest that the peptide interacts only minimally with amorphous, growing materials until a crystalline surface is generated, leading to Pd4-specific binding to control both structure and function. Such results suggest that peptides could be designed to achieve atomic-level control of NPs to allow for the engineering of both structure and functionality into materials.

The Pd4 peptide, isolated via phage display employing a Pd nanopowder target, was used for the production of peptide-capped Pd NPs using standard approaches.[4,6] In this system, the Pd4 peptide and K_2PdCl_4 were mixed in water at Pd:peptide ratios between 0 and 5, holding the peptide concentration constant. After a 30 min incubation time, the materials were reduced with a 10-fold excess of $NaBH_4$ to induce NP formation. The synthesis was fully monitored using UV−vis, high-resolution transmission electron microscopy (HR-TEM), circular dichroism (CD), ζ-potential analysis, and X-ray absorption fine structure (XAFS) spectroscopy, while the catalytic properties were analyzed via Stille coupling.

UV−vis studies of the materials synthesis are shown in Figure 1 at Pd:peptide ratios up to 4. Figure 1a presents the Pd^{2+}/peptide complex prior to reduction, where the black spectrum is derived from the materials prepared with a ratio of 1. Here, a ligand-to-metal charge-transfer (LMCT) band is observed at 215 nm, consistent with Pd^{2+} binding by the peptide amines.[7] As the Pd:peptide ratio is increased, the intensity of the LMCT band also increases; however, a second absorbance at 235 nm is observed for the system with a ratio of 4. This new absorbance is likely due to free Pd^{2+} in solution.[7] At higher ratios, the 235 nm band

Received: April 22, 2011
Published: July 21, 2011

dx.doi.org/10.1021/ja203726n | J. Am. Chem. Soc. 2011, 133, 12346–12349

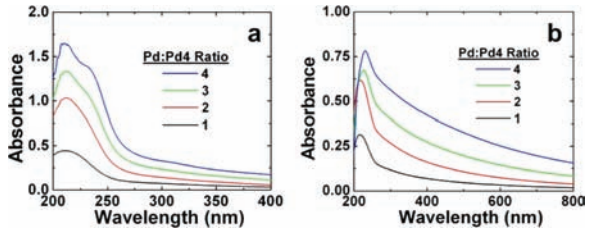

Figure 1. UV−vis analysis of the materials (a) before and (b) after reduction with $NaBH_4$.

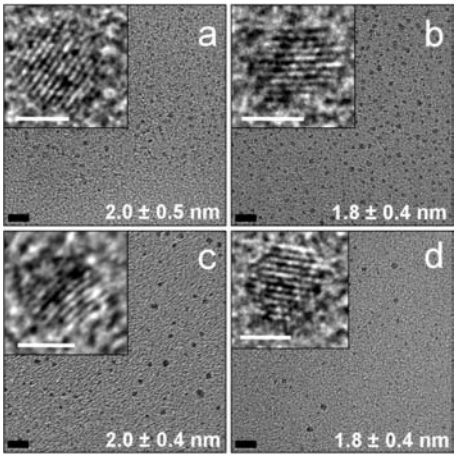

Figure 2. TEM analysis of the materials prepared at a Pd:peptide ratio of (a) 1, (b) 2, (c) 3, and (d) 4. Black scale bar = 10 nm; white scale bar (insets) = 2 nm.

increases in intensity while the LMCT band remains constant, suggesting that the peptide is saturated with Pd^{2+} at a ratio of ~4.

After reduction of the Pd^{2+}/peptide complex, the LMCT band disappears and is replaced by a spectrum with a broad absorbance band that increases in intensity toward lower wavelengths. This change indicates reduction of Pd^{2+} to form Pd^0 NPs.[4,7] Furthermore, the magnitude of the intensity of the absorbance is directly proportional to the Pd:peptide ratio used during the synthesis. For instance, the materials prepared at a ratio of 1 demonstrated the smallest absorbance intensity, which increased to the maximum absorbance observed for the materials fabricated with a ratio of 4. Such changes could result from the formation of larger Pd NPs at higher ratios or from the generation of the same sized materials for all samples whose concentration is proportional to the Pd:peptide ratio. Reduction of the materials prepared at a ratio of ≥5 resulted in bulk precipitation; thus, all studies were completed at lower ratios.

Confirmation of changes to the particle morphology were observed using TEM analysis. Figure 2a displays the materials prepared at a Pd:peptide ratio of 1, where NPs with an average size of 2.0 ± 0.5 nm were observed. The inset displays the HR-TEM image, where a single-crystal Pd NP is displayed with lattice fringes of 2.3 Å, consistent with the *d*-spacing of the Pd {111} plane.[8] Interestingly, as the Pd:peptide ratio increased, single-crystal NPs were prepared for each sample with equivalent particle sizes. For instance, at ratios of 2, 3, and 4, particle sizes of 1.8 ± 0.4, 2.0 ± 0.4, and 1.8 ± 0.4 nm were observed, respectively. These observations were highly surprising, as previous studies have demonstrated that, as the metal concentration

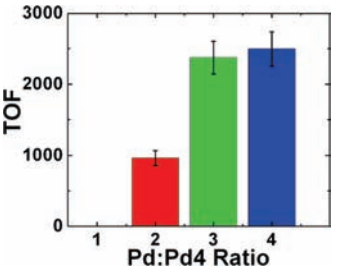

Figure 3. Catalytic analysis of the peptide-capped materials.

is increased, larger particles are prepared following standard NP nucleation and growth kinetics.[9] Furthermore, the single-crystal structure of the inorganic materials indicates that a highly controlled process is occurring to prevent defect formation. Together, this suggests that Pd4 binding of the Pd surface occurs at a very specific time point during particle growth where similar atomic-level structures are presented to the solution to produce single-crystal NPs of identical sizes.

Analysis of the NPs using ζ-potential and CD (Supporting Information, Figures S2 and S3) indicated that all materials possessed similar surface structures. Using ζ-potential, the particles prepared with a ratio of 1 possessed a surface charge of −28.6 ± 1.5 mV that decreased slightly to −36.7 ± 1.5 mV for the NPs prepared at a ratio of 4. Such slight changes are likely due to differences based upon solution ionic strength, thus suggesting that the materials possess similar bio/nano surface structures. Additionally, CD studies showed that the Pd4 peptide retained a random coil structure on the NP surface over all ratios examined. For the complexes before reduction, the peptides were less random coil-like and contained more β-turns at higher Pd^{2+}:peptide ratios. This is consistent with metal ion-induced folding of peptides, further confirming Pd^{2+}/peptide complexation; however, for all reduced species, the peptide maintained a random coil conformation on the NP surface. This suggests that the peptide/Pd surface interaction is equivalent for all of the particles, independent of the Pd^{2+} concentration.

To ascertain the effects of the synthetic variations on the catalytic activity of the materials, Stille C−C coupling between 4-iodobenzoic acid and $PhSnCl_3$ to produce biphenylcarboxylic acid (BPCA) was monitored.[2a,4] Employing the peptide-capped materials prepared at a ratio of 4 with a Pd loading of 0.05 mol %, a turnover frequency (TOF) of 2496 ± 252 mol of BPCA (mol of Pd·h)$^{-1}$ was achieved (Figure 3). This value is consistent with previous values for materials prepared at a ratio of 3.3.[2a,4] For the materials prepared at a ratio of 3, the TOF value remained constant at 2374 ± 232 mol of BPCA (mol of Pd·h)$^{-1}$; however, a decreased TOF of 965 ± 105 mol of BPCA (mol of Pd·h)$^{-1}$ was observed for the particles generated at a ratio of 2. Furthermore, nominal catalytic activity was observed for the NPs prepared at a ratio of 1, so a TOF was not determined, while minimal activity was detected for these materials over 24 h. BPCA production was noted after 48 h, suggesting that the reaction does occur, but at a slower rate.

To achieve the fabrication of consistently sized, single-crystal materials at different Pd concentrations, the Pd4 peptide must bind to the inorganic surface at a precise point during particle growth. Before reduction, a strong interaction between the Pd^{2+} and peptide amines drives the formation of a complex that is visible by UV−vis and CD. After reduction, this strong interaction is broken, leading to Pd^0 nucleation. Only weak peptide

interactions with the small nuclei likely exist to allow for particle growth. Once the particle reaches a critical size, the peptide affinity is likely to increase, resulting in surface binding. A logical point for binding to occur would be when the particle crystallizes to display the face-centered cubic (fcc) structure from which the Pd4 was isolated to bind. Since the particles are single crystals, such atomic arrangements are displayed at identical times during particle growth; thus, peptide binding would occur at the same time for each sample. During NP synthesis, the initial nucleation event is followed by a slower particle growth phase. Small nuclei are unlikely to display fcc crystallinity, due to the limited number of Pd atoms in the cluster, and would potentially not be recognized by the peptide, which is programmed to bind fcc Pd due to the phage isolation method. As the particles grow, facets would be developed along the NP surface at a critical size where the particle finally achieves the fcc structure, which may be modified by the peptide in solution. Once the materials achieve this morphology, the peptide binds, passivating the surface and capping growth. In addition, specificity of the sequence is required for binding; substitution with other peptides, such as Au binding peptides,[10] results in bulk Pd precipitation. Such a mechanism would require the production of single-crystal NPs, which are observed. Furthermore, no change in NP size would be anticipated based upon the Pd concentration.

Here, regardless of the metal concentration, Pd surface binding is dictated by precise bio/inorganic recognition, which is likely programmed during phage display.[4] As a result, at the lowest Pd:peptide ratio, excess peptide would remain in solution; however, at the higher ratios, more NPs would be produced, exhausting the peptide supply. Eventually, the amount of peptide in solution would not be able to fully passivate the NPs, thus leading to the production of bulk materials. Indeed, at ratios ≥ 5, precipitation of Pd black was observed. As a control, K_2PdCl_4 was reduced in the absence of the Pd4 peptide, which allows for rapid nucleation and particle growth. Immediately after reduction, the Pd4 peptide was added to the reaction at a Pd:peptide ratio of 4 to stabilize the growing materials. In this event, Pd NPs are stabilized with an average size of 2.5 ± 0.5 nm, which is a significant increase in diameter compared to that obtained via the standard approach (1.8 ± 0.4 nm). Larger sizes are achieved as the peptide was not in solution to arrest growth at the initial crystallization point, thus allowing the crystalline particles to continue growing. When the peptide is finally added, it rapidly binds the fcc Pd surface to cap growth, correlating well with the crystalline-based capping mechanism.

Molecular dynamics (MD) simulation with the CHARMM-METAL force field[11] shows that Pd NPs require a critical size to form stable facets (Figure 4 and SI). Both a minimum size of the particles and stable facets appear critical for Pd4 binding. Small NPs of 1.0 nm consist of only 36 atoms and exhibit a dynamically changing, non-fcc structure that could be easily influenced by the peptide (Figure 4a). The particle is smaller than the peptide and cannot develop stable, soft epitaxial interactions.[12] An increase in NP size to 1.5 nm increases the number of atoms to 120, increasing cohesion significantly within the particle as well as potential peptide attraction. A non-fcc structure close to spherical geometry was thermodynamically favored (Figure 4b) over an fcc structure of six atomic layers by 0.5 kcal/mol. The non-fcc structure was preferred upon annealing at 800 K and during a microsecond MD simulation at 298 K. The limited size and absence of defined fcc facets are not optimal for soft epitaxial binding and particle enclosure by the peptide. A further increase in particle size to 2 nm finally leads to a stable fcc particle that is bounded by {111}

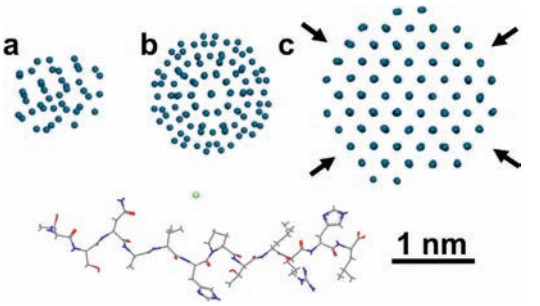

Figure 4. Equilibrium models of Pd NPs of (a) 1, (b) 1.5, and (c) 2 nm size from MD simulation at 298 K. A transition from non-fcc to fcc structure at ~2 nm leads to {111} facets (black arrows) that can be stabilized by the Pd4 peptide to inhibit particle growth. A model of the peptide (with Cl^- ion) is also shown to-scale.

facets (Figure 4c). It contains 284 atoms, and a defect-free fcc structure is also preserved upon annealing (800 K) and cooling in the simulation. The peptide then coordinates with the locally planar {111} facets and stabilizes the particle through soft epitaxial interactions described earlier.[12] Similarly, a larger NP of 3 nm diameter contains 960 atoms and is equally bound by stable {111} facets for Pd4 binding. As the appropriate fcc orientation for Pd4 binding is displayed for 2 nm particles, peptide binding occurs at this size to arrest growth, which is fully consistent with the experimental results. At the same time, the mechanism of self-assembly of multiple peptides on the NP surface, possible surface reconstruction, and many other aspects still require detailed studies in the future.

While identical NPs are prepared for each system, different catalytic TOF values were obtained. At the highest ratios, maximal activity is observed; however, the activity decreases for materials prepared at lower ratios. This suggests that, while the particles are identical in each sample, the overall reaction solution must be different to result in the varied TOFs. To probe the reaction mixture, Pd K-edge XAFS studies were conducted at beamline X18B at the National Synchrotron Light Source at Brookhaven National Laboratory. For this analysis, the Pd NPs prepared at the selected Pd:peptide ratios were synthesized and dried via lyophilization. The powders were then spread on adhesive tape, and their X-ray absorption coefficient was measured in transmission mode between 150 eV below and 1350 eV above the Pd K-edge (24 353 eV). As shown in Figure 5a,b, the X-ray Absorption Near Edge Structure (XANES) data demonstrate a strong similarity between all samples and a contrast with bulk Pd foil used as a control. Figure 5b presents an expanded analysis at the near edge features, which demonstrates isosbestic points at 24384 and 24399 eV for the NP samples. This suggests that the reaction samples contain a mixture of two Pd components that vary proportionally to the ratio used during synthesis. After the background subtraction and edge-step normalization, the extended XAFS (EXAFS) data for the four samples were converted to *k*-space, k^2-weighted, and Fourier transformed to *r*-space. The Fourier transform magnitudes for the four NP samples are presented in Figure 5c, while data-fitting of the results for the NPs is presented in the Supporting Information, Figure S4. From the *r*-space data, the peak at ~0.25 nm (uncorrected for phase shift) arises from Pd−Pd coordination within the NP sample, while the peak at ~0.15 nm represents the Pd−O/N coordination. Unfortunately, EXAFS is unable to distinguish between N and O scatterers due to their similar Z-values; thus, the data are reported

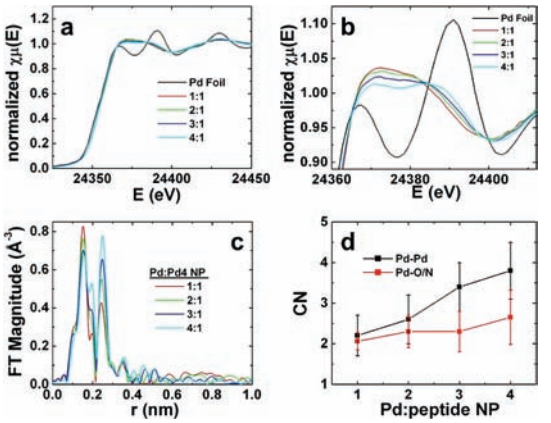

Figure 5. Pd K-edge XAFS analysis of the NPs prepared at Pd:peptide ratios of 1−4. Part (a) presents the XANES plot, while part (b) displays the narrower energy range. Part (c) presents the *r*-space analysis, while part (d) presents the trends in Pd−Pd and Pd−O/N CNs.

as O/N. As is evident, a direct correlation between the intensity of these peaks and the Pd:peptide ratio used during synthesis is present. Here, as the ratio increases, the Pd−O/N peak decreases slightly, with an increase observed in the Pd−Pd peak. The first nearest-neighbor coordination numbers (CN) for Pd−Pd and Pd−O/N obtained from EXAFS analysis of the *r*-space data are presented in Figure 5d, which confirms the increase in Pd−Pd bonds with an increase in the Pd:peptide ratio. This suggests that the percent of Pd^{2+} ions reduced in the peptide/Pd^{2+} complex is highest for the sample prepared at a ratio of 4 and is lower for the NPs generated at a ratio of 1. This suggests that a mixture of unreduced complex and reduced NPs are present in the samples, which gives rise to the isosbestic points in the absorbance data. Interestingly, the Pd−O/N value remains roughly the same throughout the analysis within error bars.

This effect of reduction is the basis for the observed catalytic results. At high ratios, more Pd^{2+} is reduced to yield more active Pd^0 materials to generate high TOFs. As the ratio decreases, less reactive Pd^0 is present; thus, lower TOFs are anticipated. This change in the percent of Pd^{2+} that is reduced is likely due to the ion coordination to the peptide, which can shift the reduction potential of the metal salt.[13] At the low ratios, the Pd^{2+} would possess the highest number of bonds to the peptide, thus shifting the reduction potential the farthest, which would make it the most difficult sample to reduce. As the ratio changes to 4, the peptide coordination of the Pd^{2+} would decrease for a more easily reduced sample. Such results are observed via EXAFS and the catalytic activity. This suggests that monitoring the materials before and after reduction is important for understanding the structure and functionality.

In conclusion, our results suggest that the Pd4 peptide employs crystallographic binding to control the size and functionality of peptide-capped Pd NPs. Once the growing NPs achieve the appropriate crystal structure, peptide surface binding occurs, resulting in the fabrication of Pd NPs of equivalent sizes. This effect was supported through theoretical modeling and catalytic analyses. These results represent a step toward elucidating the binding specificity of materials-directing peptides for their respective target surfaces. Furthermore, they suggest that peptides could be used to design highly specific NP interfaces at the atomic level, which would be attractive for the fabrication of complex inorganic materials for a wide variety of applications.

■ ASSOCIATED CONTENT

Supporting Information. Synthetic and simulation procedures, particle size histograms, control analysis, ζ-potential analysis, CD spectra, and full EXAFS analysis. This material is available free of charge via the Internet at http://pubs.acs.org.

■ AUTHOR INFORMATION

Corresponding Author
rajesh.naik@wpafb.af.mil; knecht@miami.edu

■ ACKNOWLEDGMENT

This material is based upon work supported by the National Science Foundation under Grants No. CBET-1033334 (M.K.) and DMR-0955071 (H.H.), and by the Air Office of Scientific Research (R.N.). Acknowledgement is made to the donors of the American Chemical Society Petroleum Research Fund for partial support (M.K.). A.I.F. acknowledges support by U.S. Department of Energy Grant DE-FG02-03ER15476. Beamline X18B at the NSLS is supported in part by the Synchrotron Catalysis Consortium, U.S. Department of Energy Grant No DE-FG02-05ER15688. R.C. acknowledges student fellowship support from the UK Research Challenge Trust Fund. The authors are grateful to Dr. R. Vasic for help with XAFS measurements.

■ REFERENCES

(1) (a) Wang, L.; Yang, R. T. *Energy Environ. Sci.* **2008**, *1*, 268. (b) Jain, P. K.; Huang, X.; El-Sayed, I. H.; El-Sayed, M. A. *Acc. Chem. Res.* **2008**, *41*, 1578. (c) Daniel, M.-C.; Astruc, D. *Chem. Rev.* **2004**, *104*, 293. (d) Knecht, M. R.; Pacardo, D. B. *Anal. Bioanal. Chem.* **2010**, *397*, 1137. (e) Scott, R. W. J.; Wilson, O. M.; Crooks, R. M. *J. Phys. Chem. B* **2005**, *109*, 692. (f) Astruc, D. *Inorg. Chem.* **2007**, *46*, 1884.

(2) (a) Coppage, R.; Slocik, J. M.; Sethi, M.; Pacardo, D. B.; Naik, R. R.; Knecht, M. R. *Angew. Chem., Int. Ed.* **2010**, *49*, 3767. (b) Diallo, A. K.; Ornelas, C.; Salmon, L.; Aranzaes, J. R.; Astruc, D. *Angew. Chem., Int. Ed.* **2007**, *46*, 8644.

(3) Dickerson, M. B.; Sandhage, K. H.; Naik, R. R. *Chem. Rev.* **2008**, *108*, 4935.

(4) Pacardo, D. B.; Sethi, M.; Jones, S. E.; Naik, R. R.; Knecht, M. R. *ACS Nano* **2009**, *3*, 1288.

(5) Chiu, C.-Y.; Li, Y.; Ruan, L.; Ye, X.; Murray, C. B.; Huang, Y. *Nat. Chem.* **2011**, *3*, 393.

(6) Naik, R. R.; Stringer, S. J.; Agarwal, G.; Jones, S. E.; Stone, M. O. *Nat. Mater.* **2002**, *1*, 169.

(7) Scott, R. W. J.; Ye, H.; Henriquez, R. R.; Crooks, R. M. *Chem. Mater.* **2003**, *15*, 3873.

(8) Jakhmola, A.; Bhandari, R.; Pacardo, D. B.; Knecht, M. R. *J. Mater. Chem.* **2010**, *20*, 1522.

(9) (a) Frenkel, A. I.; Nemzer, S.; Pister, I.; Soussan, L.; Harris, T.; Sun, Y.; Rafailovich, M. H. *J. Chem. Phys.* **2005**, *123*, 184701. (b) Templeton, A. C.; Chen, S.; Gross, S. M.; Murray, R. W. *Langmuir* **1999**, *15*, 66.

(10) Slocik, J. M.; Stone, M. O.; Naik, R. R. *Small* **2005**, *1*, 1048.

(11) Heinz, H.; Vaia, R. A.; Farmer, B. L.; Naik, R. R. *J. Phys. Chem. C* **2008**, *112*, 17281.

(12) (a) Heinz, H.; Farmer, B. L.; Pandey, R. B.; Slocik, J. M.; Patnaik, S. S.; Pachter, R.; Naik, R. R. *J. Am. Chem. Soc.* **2009**, *131*, 9704. (b) Feng, J.; Pandey, R. B.; Berry, R. J.; Farmer, B. L.; Naik, R. R.; Heinz, H. *Soft Matter* **2011**, *7*, 2113.

(13) Knecht, M. R.; Weir, M. G.; Myers, V. S.; Pyrz, W. D.; Ye, H.; Petkov, V.; Buttrey, D. J.; Frenkel, A. I.; Crooks, R. M. *Chem. Mater.* **2008**, *20*, 5218.